

Experimental realization of order-finding with a quantum computer

Lieven M.K. Vandersypen^{1,2,*}, Matthias Steffen^{1,2}, Gregory Breyta², Costantino S. Yannoni², Richard Cleve³,
and Isaac L. Chuang²

¹ *Solid State and Photonics Laboratory, Stanford University, Stanford, CA 94305-4075*

² *IBM Almaden Research Center, San Jose, CA 95120*

³ *Dept. of Computer Science, University of Calgary, Calgary, Alberta, Canada T2N 1N4*

(October 28, 2018)

We report the realization of a nuclear magnetic resonance (NMR) quantum computer which combines the quantum Fourier transform (QFT) with exponentiated permutations, demonstrating a quantum algorithm for order-finding. This algorithm has the same structure as Shor’s algorithm and its speed-up over classical algorithms scales exponentially. The implementation uses a particularly well-suited five quantum bit molecule and was made possible by a new state initialization procedure and several quantum control techniques.

The quest for the experimental realization of quantum computers has culminated in the creation of specific entangled quantum states, most recently with four quantum bits (qubits) using trapped ions [1], and seven qubits [2] using liquid state nuclear magnetic resonance (NMR) [3,4], and in the successful implementation of Grover’s search algorithm [5–7] and the Deutsch-Jozsa algorithm [8–10] on two, three, and five qubit systems (see [11] for additional references).

However, a key step which remains yet to be taken is a computation with the structure of Shor’s factoring algorithm [12,13], which appears to be common to all quantum algorithms that achieve exponential speed-up [14]. This structure involves two components: exponentiated unitary operations and the quantum Fourier transform (QFT). Implementing these components is challenging because they require not just the creation of *static* entangled states [1,2], but also precise *dynamic* quantum control over the evolution of multiple entangled qubits, over the course of tens to hundreds of quantum gates for the smallest meaningful instances of this class of algorithms. The evolution of the states is precisely where NMR quantum computers appear to have an exponential advantage over classical computers [15].

Here we report the experimental implementation of a quantum algorithm for finding the order of permutation [12,13,16]; its structure is the same as for Shor’s factoring algorithm and it scales exponentially faster than any classical algorithm for the problem. The realization of this algorithm was made possible by the synthesis of an unusual molecule with five pairwise coupled, easily addressable ¹⁹F spins, and by the introduction of two new techniques: an efficient and effective temporal labeling scheme for initial state preparation, and a method for precise simultaneous rotations of multiple spins at nearby frequencies [17].

The order of a permutation π can be understood via the following analogy: imagine 2^n rooms and 2^n *one-way* passages connecting the rooms, with *exactly* one entrance and one exit in each room (for some rooms, the passage going out may loop back to the room itself). These rules

ensure that when making transitions from one room to the next going through the passages, you must eventually come back to the room you started from. Define the order r as the *minimum* number of transitions needed to return to the starting room y , where r may depend on y . The order-finding problem is to determine r solely by trials of the type “make x transitions using π starting from room y and check which room you are in”. Mathematically, we will describe such trials as queries of an oracle or black box which outputs $\pi^x(y)$. The goal then is to find r with the least possible number of queries.

Cleve showed that order-finding using no other resource or information than the oracle is hard both for deterministic and probabilistic classical computers [18], i.e. there exists a lower bound on the number of oracle queries needed for order-finding which is exponential in n . In contrast, this problem can be solved much faster on a quantum computer, because finding the order of $\pi(y)$ is equivalent to finding the period of the function $f(x) = \pi^x(y)$. The latter can be done with a constant probability of success in a constant number of function evaluations using a generalization of Shor’s quantum algorithm [16]. This is because, in some sense, the quantum computer can make transitions to many rooms at once. Thus, in terms of the number of oracle queries required, the gap between the quantum and classical case is exponential [18].

We experimentally implemented the order-finding quantum algorithm to determine the order of a representative subset of all $4! = 24$ permutations on 4 elements, including instances of each possible order. It can be proven that the best classical algorithm needs two queries of the oracle to determine r with certainty, and that using only one query of the oracle, the probability of finding r using a classical algorithm can be no more than $1/2$. One optimal classical strategy is to first ask the oracle for the value of $\pi^3(y)$: when the result is y , r must be 1 or 3; otherwise r must be 2 or 4. In either case, the actual order can be guessed only with probability $1/2$. In contrast, the probability of success is ~ 0.55 with only one oracle-query using the quantum algorithm on a single

quantum computer. In fact, since in our implementation an ensemble of $\sim 10^{18}$ quantum computers contribute to the signal, our output data enables the order to be deduced with virtual certainty.

The quantum algorithm is as follows (see Fig. 1 for the quantum circuit): **(0)** initialize the first register of three qubits in the state $|0\rangle$ and set the second register of two qubits to $|y_1y_0\rangle$ or for short $|y\rangle$, where y_1y_0 is the binary representation of the number y ; **(1)** apply a Hadamard transform H to qubits 1, 2 and 3, which puts the first register in the state $|x\rangle = (|0\rangle + |1\rangle + \dots + |7\rangle)/\sqrt{8}$; **(2)** apply the unitary transformation $|x\rangle|y\rangle \mapsto |x\rangle|\pi^x(y)\rangle$, which is the oracle query; **(3)** perform the quantum Fourier transform (QFT) on the first three qubits [19]; **(4)** measure the first three qubits — for an ideal single quantum computer, the possible measurement outcomes m and their probabilities are listed in Fig. 2 for each possible value of r (the translation to ensemble averaged measurements is discussed later); **(5)** depending on the measurement outcome, make a probabilistic guess r' as shown also in Fig. 2. It is easy to verify that $\Pr[r' = r]$ is ~ 0.55 , regardless of the probability distribution of r or π .

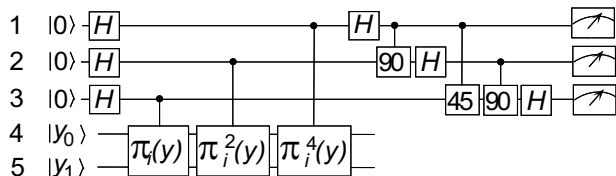


FIG. 1. The quantum circuit for order-finding. Horizontal lines represent qubits; time goes from left to right. The boxed 90 and 45 represent rotations about \hat{z} over those angles. A black dot connected to a box on another horizontal line indicates that the boxed operation is executed if and only if the qubit indicated by the black dot is $|1\rangle$. The transformation $|x\rangle|y\rangle \mapsto |x\rangle|\pi^x(y)\rangle$ (step 2) was implemented in three steps, using the fact that $\pi^x = \pi^{x_0}\pi^{2x_1}\pi^{4x_2}$, where $x_2x_1x_0$ is the binary representation of x . Each of these three operations is a permutation on qubits 4 and 5, controlled by qubits 3, 2 and 1 respectively. The details of the controlled permutations depend on π . The QFT (step 3) was implemented using the construction of [20], which swaps the output state of qubits 1 and 3 compared to the definition of the QFT.

m	$r=1$	$r=2$	$r=3$	$r=4$	r'	$m=0$	$m=\text{odd}$	$m=2,6$	$m=4$
0	1	0.5	0.34375	0.25	1	0.5505	0	0	0
1,7	0	0	0.01451	0	2	0.1009	0	0	1
2,6	0	0	0.0625	0.25	3	0.1468	1	0	0
3,5	0	0	0.23549	0	4	0.2018	0	1	0
4	0	0.5	0.03125	0.25					

FIG. 2. (Left) The probabilities that the measurement result m is 0, 1, \dots , or 7, given r (for an ideal single quantum computer). (Right) The optimal probabilities with which to make a guess r' for r , given m .

In order to implement this algorithm, we custom synthesized a molecule [21] containing five ^{19}F spins which served as the qubits (Fig. 3). When placed in a static

magnetic field, each spin has two discrete energy eigenstates, spin-up, $|0\rangle$, and spin-down, $|1\rangle$, described by the Hamiltonian $\hbar\omega_i I_{z_i}$, where ω_i is the transition frequency between the spin-up and spin-down states and I_z is the \hat{z} component of the spin angular momentum operator. In this molecule, *all* five spins are remarkably well-separated in frequency, ω_i , and are mutually coupled with a coupling Hamiltonian of the form $2\pi\hbar J_{ij} I_{z_i} I_{z_j}$ (Fig. 3). The linewidths of the NMR transitions are ~ 1 Hz, so the T_2 quantum coherence times of the spins were at least ~ 0.3 s. The T_1 time constants were measured to be between 3 and 12 s.

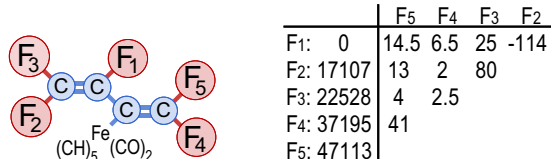


FIG. 3. Structure of the pentafluorobutadienyl cyclopentadienyldicarbonyliron complex, with a table of the relative chemical shifts of the ^{19}F spins at 11.7 T [Hz], and the J -couplings [Hz]. A total of 76 out of the 80 lines in the 5 spectra are resolved.

This nuclear spin system was used at room temperature. The thermal equilibrium state is then highly mixed, i.e. the probabilities that each spin is $|0\rangle$ or $|1\rangle$ differ by only 1 part in $\sim 10^5$, which is not a suitable initial state for a quantum computation [22]. Instead, as has previously been shown, an “effective pure” initial state must be created, in which only the spins in the $|00000\rangle$ state produce a net output signal [3,4]. We devised a new procedure to prepare effective pure states which is best understood in terms of product operators [23]. The equilibrium density matrix for a homonuclear spin system is a sum of $n = 5$ terms: $IIIIZ + IIIZI + IIZII + IZIII + ZIIII$. The desired effective pure state density matrix is $IIIIZ + \dots + ZIIII + IIIZZ + \dots + ZZIII + IZZZZ + \dots + ZZZII + IZZZZ + \dots + ZZZZI + ZZZZZ$, a sum of $2^n - 1 = 31$ terms. Using short sequences of controlled-NOT operations (C_{ij} flips spin j if and only if i is $|1\rangle$), the five terms obtained in equilibrium can be transformed into different sets of five terms. For homonuclear spin systems, the summation of only $\lceil (2^n - 1)/n \rceil = 7$ different experiments thus suffices to create all 31 terms, although it may be advantageous to use slightly more experiments in order to keep the preparation sequences short. In contrast, both conventional temporal averaging [24] and later improvements [7] require up to $2^n - 1$ experiments, and furthermore suffer from higher complexity and/or a lower signal-to-noise ratio. The overhead is still exponential though, so even this improved technique is not scalable. But importantly, a scalable approach to NMR quantum computation exists [25] and may become practical if large polarization enhancements can be achieved. We used 9 experiments, giving a total of 45 product operator terms. The 14 extra terms

were canceled out pairwise, using NOT (N_i) operations to flip the sign of selected terms. The 9 state preparation sequences were

$$\begin{aligned} & C_{51}C_{45}C_{24}N_3, C_{14}C_{31}C_{53}N_2, C_{54}C_{51}N_2, \\ & C_{31}C_{43}C_{23}N_5, C_{21}C_{52}C_{45}C_{34}, C_{53}C_{25}C_{12}N_4, \\ & C_{12}C_{15}C_{13}C_{41}, C_{32}C_{13}C_{25}N_4, C_{35}C_{23}N_1. \end{aligned}$$

The resulting data are remarkably clean, as illustrated in Fig. 4. After the state preparation, only the 0000 line should remain visible, reflecting that only molecules with all spins in the ground state contribute to the signal. This is clearly observed in the measured spectra.

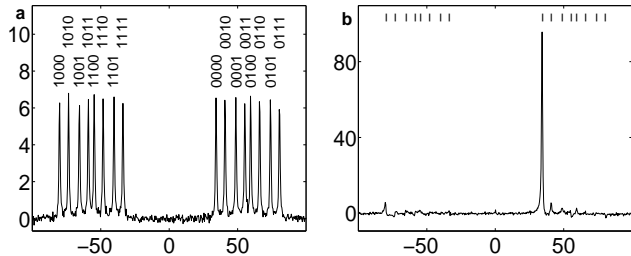


FIG. 4. All spectra shown here and in Fig. 5 display the real part of the spectrum in the same arbitrary units, and were obtained without phase cycling or signal-averaging (except for Fig. 5 c, where 16 identical scans were averaged). A 0.1 Hz filter was applied. Frequencies are in units of Hz with respect to ω_1 . **a**, the spectrum of spin 1 in equilibrium. The 16 lines are due to shifts in the transition frequency ω_1 by $\pm J_{1,j}/2$, depending on whether spin j is in $|0\rangle$ or $|1\rangle$. In equilibrium, all the 32 states are nearly equally populated, hence the 16 lines in each spectrum have virtually the same intensity. Taking into account the sign and magnitude of the $J_{1,j}$, the 16 lines in the spectrum of spin 1 can be labeled as shown. **b**, the same spectrum when the spins are in an effective pure state. Only the line labeled 0000 is present.

This effective pure state served as the initial state for the order-finding algorithm. The actual computation was realized via a sequence of ~ 50 to ~ 200 radio-frequency (RF) pulses, separated by time intervals of free evolution under the Hamiltonian, for a total duration of ~ 50 to ~ 500 ms, depending on π . The pulse sequences for the order-finding algorithm were designed by translating the quantum circuits of Fig. 1 into one- and two-qubit operations, employing several simplification methods [7]. These pulse sequences were implemented on a custom modified four-channel Varian Unity INOVA spectrometer, and a Nalorac HFX probe. The frequency of one channel was set at $(\omega_2 + \omega_3)/2$, and the other three channels were set on the resonance of spins 1, 4 and 5. The chemical shift evolutions of spins 2 and 3 were calculated with the help of a time-counter, which kept track of the time elapsed from the start of the pulse sequence. On-resonance excitation of spins 2 and 3 was achieved using phase-ramping techniques [26]. All pulses were spin-selective and Hermite shaped [23]. Rotations about the \hat{z} -axis were implemented by adjusting the phases of the subsequent pulses [23]. Unintended phase shifts [27]

of spins i during a pulse on spin $j \neq i$ were calculated and accounted for by adjusting the phase of subsequent pulses. During simultaneous pulses, the effect of these phase shifts was largely removed by shifting the frequency of the pulses via phase-ramping. The pulse frequency shifts are designed such that they track the shifting spin frequencies and thereby greatly improve the accuracy of the simultaneous rotations of two or more spins [17]. This technique circumvents the need to avoid simultaneous pulses at nearby frequencies [28], and thus permits more efficient pulse sequences.

Upon completion of the pulse sequence, the states of the three spins in the first register were measured and the order r was determined from the read-out. Since an ensemble of quantum computers rather than a single quantum computer was used, the measurement gives the bitwise average values of $m_i (i = 1, 2, 3)$, instead of a sample of $m = m_1 m_2 m_3$ with probabilities given in Fig. 2 [29]. Formally, measurement of spin i returns $O_i = 1 - 2\langle m_i \rangle = 2\text{Tr}(\rho I_{zi})$, where ρ is the final density operator of the system. The O_i are obtained experimentally from integrating the peak areas in the spectrum of the magnetic signal of spin i after a 90° read-out pulse on spin i , phased such that positive spectral lines correspond to positive O_i . The theoretically predicted values of $O_i (i = 1, 2, 3)$ for each value of r follow directly from the probabilities for m in Fig. 2. For reference, we also include the values of O_4 and O_5 (for $y = 0$; if $y \neq 0$, O_4 and O_5 can be negative): for the case $r = 1$ the O_i are 1, 1, 1, 1, 1; for $r = 2$ they are 1, 1, 0, 1, 0; and for $r = 4$ they are 1, 0, 0, 0, 0. For $r = 3$, the $O_i (i = 1, 2, 3)$ are 0, $1/4$, $5/16$, and O_4 and O_5 can be 0, $\pm 1/4$ or $\pm 1/2$, depending on y . The value of r can thus be unambiguously determined from the spectra of the three spins in the first register. This was confirmed experimentally by taking spectra for these three spins, which were in excellent agreement with the theoretical expectations.

In fact, the complete spectrum of any one of the first three spins uniquely characterizes r by virtue of extra information contained in the splitting of the lines. For the spectrum of spin 1 the values of O_i given above indicate that for $r = 1$, only the 0000 line (see Fig. 4) will be visible since spins 2 – 5 are all in $|0\rangle$. Furthermore, this line should be absorptive and positive since spin 1 is also in $|0\rangle$. Similarly, for $r = 2$ the 0000, 0001, 0100 and 0101 lines are expected to be positive, and for $r = 4$ all 16 lines should be positive. Finally, for $r = 3$, the *net* area under the lines of spin 1 should be zero since $O_1 = 0$, although most individual lines are expected to be non-zero and partly dispersive. These unambiguous characteristics are reflected in the data. Results for four representative permutations are presented in Fig. 5. In all cases, the spectrum is in good agreement with the predictions, both in terms of the number of lines, and their position, sign and amplitude. Slight deviations from the ideally expected spectra are attributed mostly to incom-

plete refocusing of undesired coupled evolutions and to decoherence.

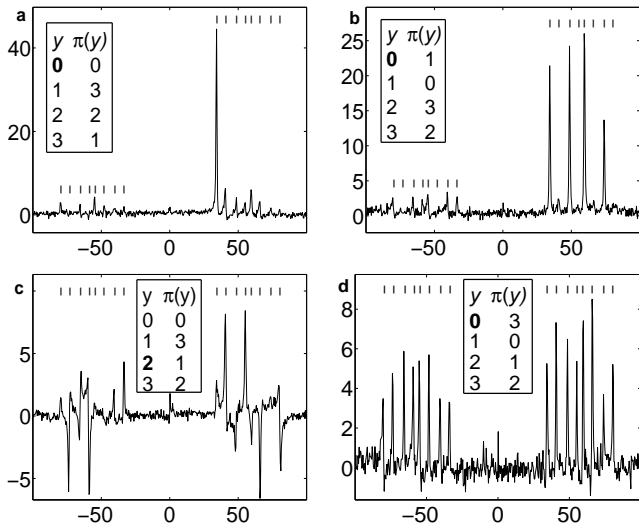


FIG. 5. Spectra of spin 1 acquired after executing the order-finding algorithm. The respective permutations are shown in inset, with the input element highlighted. The 16 marks on top of each spectrum indicate the position of the 16 lines in the thermal equilibrium spectrum. The transformation $|x\rangle|y\rangle \mapsto |x\rangle|\pi^x(y)\rangle$ is realized by **a**, $r = 1$: $P_{54} C_{35} P_{54}^\dagger C_{35} P_{34}$ (P_{ij} rotates spin j by 90° about \hat{z} if and only if spin i is $|1\rangle$). **b**, $r = 2$: C_{35} . **c**, $r = 3$: $C_{32} C_{25} C_{32} C_{21} P_{14} C_{51} P_{14}^\dagger C_{51} P_{54} C_{21} P_{15} C_{41} P_{15}^\dagger C_{41} P_{45}$. (this sequence does the transformation $\pi^x(y)$ for $y = 2$ only; sequences for $r = 3$ that would work for any y are prohibitively long). **d**, $r = 4$: $C_{24} P_{34} P_{54} C_{35} P_{54}$. Each transformation was tested independently to confirm its proper operation.

The success of the order-finding experiment required the synthesis of a molecule with unusual NMR properties and the development of several new methods to meet the increasing demands for control over the spin dynamics. The major difficulty was to address and control the qubits sufficiently well to remove undesired couplings while leaving select couplings active. Furthermore, the pulse sequence had to be executed within the coherence time. Clearly, the same challenges will be faced in moving beyond liquid state NMR, and we anticipate that solutions such as those reported here will be useful in future quantum computer implementations, in particular in those involving spins, such as solid state NMR [30], electron spins in quantum dots [31] and ion traps [1].

We thank X. Zhou, A. Verhulst, M. Sherwood, S. Smallcombe, A. Brooke and R. Laflamme for help and discussions, J. Harris and W. Risk for support, and the Aspen Center for Physics for its hospitality. L.V. gratefully acknowledges support by a Yansouni Family Stanford Graduate Fellowship. This work was supported by DARPA under the NMRQC initiative.

* Email address: lieven@snow.stanford.edu.

[1] C.A. Sackett *et al.*, Nature **404**, 256 (2000).

[2] E. Knill, R. Laflamme, R. Martinez and C.-H. Tseng, Nature **404**, 368 (2000). However, in current room temperature NMR experiments, entangling operations are performed on a density matrix so close to the identity matrix that the state remains separable, as shown by S.L. Braunstein *et al.*, Phys. Rev. Lett. **83**, 1054 (1999).

[3] N. Gershenfeld and I.L. Chuang, Science **275**, 350 (1997).

[4] D.G. Cory, A.F. Fahmy, and T.F. Havel, Proc. Nat. Acad. Sci. **94**, 1634 (1997).

[5] I.L. Chuang, N. Gershenfeld, and M. Kubinec, Phys. Rev. Lett. **80**, 3408 (1998).

[6] J.A. Jones, M. Mosca and R.H. Hansen, Nature **393**, 344 (1998).

[7] L.M.K. Vandersypen *et al.*, Appl. Phys. Lett. **76**, 646 (2000).

[8] I.L. Chuang, L.M.K. Vandersypen, X. Zhou, D.W. Leung, and S. Lloyd, Nature **393**, 143 (1998).

[9] J.A. Jones and M. Mosca, J. Chem. Phys. **109**, 1648 (1998).

[10] R. Marx *et al.*, Phys. Rev. A **62** 012310 (2000).

[11] J.A. Jones, to appear in Fortschritte der Physik special issue, Experimental Proposals for Quantum Computation, quant-ph/0002085.

[12] P. Shor, Proc. 35th Ann. Symp. on Found. of Comp. Sci., p. 124 (IEEE Comp. Soc. Press, Los Alamitos, CA, 1994).

[13] A. Ekert and R. Jozsa, Rev. of Mod. Phys. **68**, 733 (1996).

[14] R. Cleve, A. Ekert, C. Macchiavello and M. Mosca, Proc. R. Soc. Lond. A **454**, 339 (1998).

[15] R. Schack and C.M. Caves, Phys. Rev. A **60**, 4354 (1999).

[16] A.Y. Kitaev, quant-ph/9511026.

[17] M. Steffen, L.M.K. Vandersypen, and I.L. Chuang, J. Magn. Reson. **146**, 369 (2000).

[18] R. Cleve, Proc. 15th Ann. IEEE Conf. on Computational Complexity (IEEE Computer Society Press, Los Alamitos, CA, 2000), p. 54.

[19] Y.S. Weinstein, S. Lloyd and D.G. Cory, quant-ph/9906059.

[20] D. Coppersmith, IBM Research Report RC19642 (1994).

[21] M. Green, N. Mayne, and F.G.A. Stone, J. Chem. Soc. (A), 902 (1968).

[22] If r were independent of the value of y , the second register would not have to be prepared in an effective pure state, but in general r may depend on y so all five spins were made effective pure in all spectra shown.

[23] R. Freeman, *Spin Choreography* (Spektrum, Oxford, 1997).

[24] E. Knill, I.L. Chuang, and R. Laflamme, Phys. Rev. A **57**, 3348 (1998).

[25] L.J. Schulman and U.V. Vazirani, Proc. 31st Ann. ACM Symp. Theory of Computing, 1999, Atlanta, GA, p. 322.

[26] S.L. Patt, J. Magn. Reson. **96**, 94 (1992).

[27] L. Emsley, and G. Bodenhausen, Chem. Phys. Lett. **168**, 297 (1990).

[28] N. Linden, Ě Kupĉe, and R. Freeman, Chem. Phys. Lett. **311**, 321 (1999).

[29] It is not clear, however, that the bitwise average outputs of the QFT suffice to determine r for permutations on arbitrary n . Instead, classical post-processing on the quantum computer [3] can be used to compute r .

[30] B.E. Kane, Nature **393**, 133 (1998).

[31] D. Loss and D. DiVincenzo, Phys. Rev. A **57**, 120 (1998).